

Fuzzy based damping controller for TCSC using local measurements to enhance transient stability of power systems



Mohsen Bakhshi, Mohammad Hosein Holakooie, Abbas Rabiee*

Department of Electrical Engineering, University of Zanjan, Zanjan, Iran

ARTICLE INFO

Article history:

Received 2 December 2015

Received in revised form 14 May 2016

Accepted 28 June 2016

Keywords:

Fuzzy controller

Local measurements

Thyristor controlled series capacitor (TCSC)

Transient stability

Wide-area measurements

ABSTRACT

This paper proposes a local fuzzy based damping controller (LFDC) for thyristor controlled series capacitor (TCSC) to improve transient stability of power systems. In order to implement the proposed scheme, detailed model of TCSC, based on actual behavior of thyristor valves, is adopted. The LFDC uses the frequency at the TCSC bus as a local feedback signal, to control the firing angle. The parameters of fuzzy controller are tuned using an off-line method through chaotic optimization algorithm (COA). To verify the proposed LFDC, numerical simulations are carried out in Matlab/Simpower toolbox for the following case studies: two-area two-machine (TATM), WSCC three-machine nine-bus and Kundur's two-area four-machine (TAFM) systems under various faults types. In this regard, to more evaluate the effectiveness of the proposed method, the simulation results are compared with the wide-area fuzzy based damping controller (WFDC). Moreover, the transient behavior of the detailed and phasor models of the TCSC is discussed in the TATM power system. The simulation results confirm that the proposed LFDC is an efficient tool for transient stability improvement since it utilizes only local signals, which are easily available.

© 2016 Elsevier Ltd. All rights reserved.

1. Introduction

Flexible AC transmission systems (FACTS) devices are effective tools to enhance power transmission capability, stability margin and voltage profile. Among various types of FACTS devices, thyristor controlled series capacitor (TCSC) is an economical and efficient choice to improve dynamic behavior of interconnected power systems via fast and smooth variation of the transmission line reactance [1–4].

Different applications of TCSC have been widely addressed in technical literature, which confirm capability of TCSC in the face of detrimental phenomena such as transient instability and subsynchronous resonance (SSR). The series capacitor inherently raises the probability of SSR problem. In this regard, a number of articles have developed the structure of TCSC controller to eliminate the SSR problem [5–7]. In order to improve small signal stability and damping of both local and inter-area electromechanical oscillations, power system stabilizer (PSS) is vastly used as the first choice [8]. On the other hand, in the recent years coordination between PSS and various types of FACTS devices has been examined as an alternative methodology instead of conventional PSS-

based damping controllers. To address the mentioned subject, supplementary damping controllers (SDCs) are presented in [9–11]. Moreover, the robust H_∞ damping controller is developed in [12]. A TCSC fuzzy damping controller based on transient energy function is discussed in [13]. Ref. [14] proposes the self-tuning fuzzy PI controller for enhancement of power system stability. Improvement of power system transient stability is another advantage of the TCSC. In Ref. [15], the authors studied transient stability by using trajectory sensitivity analysis in multi-machine power systems. In addition, transient stability has been improved using an artificial neural network and T-S model based fuzzy controller for TCSC in [16,17] respectively. It should be noted that the majority of researches in association with the TCSC have utilized simplified equivalent models such as linear and phasor models for TCSC, while the actual impacts of thyristor switches on the TCSC behavior have been neglected.

The TCSC input signals are usually divided into two main categories, local and remote signals. The remote signals require fast and safe communication infrastructure, which regardless of employing the modern communication systems, the communication failure is an inseparable feature of these systems [18]. Wide area measurement system (WAMS) is an interesting technology, which is based on synchronous phasor measurements and communication channels for implementation of wide area controllers (WACs). However, this technology is inherently suffered from time

* Corresponding author.

E-mail addresses: m.bakhshi@znu.ac.ir (M. Bakhshi), hosein.holakooie@znu.ac.ir (M.H. Holakooie), rabiee@znu.ac.ir (A. Rabiee).

delay, which impresses the stability and reliability of the system. Moreover, determination of the maximum allowable time delay is another challenge for the WAC-based power systems [19].

This paper proposes a local fuzzy based damping controller (LFDC) for TCSC to enhance the transient stability of multi-machine power systems. The employed local control signal is the frequency of the voltage at the TCSC installed bus, which is dependably available. In order to verify the performance of proposed LFDC scheme, it is compared with wide-area fuzzy based damping controller (WFDC). Since, wide-area measurements are available after a certain time delay, and due to the failure of communication infrastructures, the performance of WFDC scheme is analyzed and compared with the proposed LFDC in the presence of such practical limitations. The comparative results of the LFDC and WFDC in different test systems substantiate that the proposed LFDC can satisfy the desired performance under different types of faults. Furthermore, the detailed model of TCSC is implemented, which gives more realistic results than its conventional phasor model. Briefly, the main contributions of this paper are:

- Utilization of local signal (frequency at the TCSC bus) instead of wide-area signal (rotor-speed) to design TCSC damping controller.
- Implementation of detailed model of TCSC and surveying the effect of this model on the behavior of power system low frequency oscillations.
- Developing a fuzzy controller with optimized coefficients using COA algorithm.
- Presenting a complete comparative study to examine the performance of the proposed LFDC scheme in different case studies for normal condition and different communication links delays and failures.

The rest of this paper is organized as follows. Section 2 introduces the detailed model of TCSC. Section 3 describes the proposed LFDC which includes the preliminary remarks, the fuzzy controller and the chaotic optimization algorithm (COA). Case studies and simulation results are presented in Sections 4 and 5, respectively. Finally, Section 6 summarizes the findings and concludes the paper.

2. Detailed model of TCSC

The TCSC is usually composed of a fixed capacitor (FC) in parallel with a thyristor controlled reactor (TCR). The TCR consists of bi-directional and anti-parallel thyristor valves in series with a reactor. In power system stability studies, the TCSC increases the stability margin by manipulating the equivalent series reactance of transmission line. The fundamental frequency reactance of the TCSC is calculated as follows [2]:

$$X_{TCSC} = X_C - \frac{X_C^2}{X_C - X_L} \cdot \frac{2\beta + \sin(2\beta)}{\pi} + \frac{4X_C^2}{X_C - X_L} \cdot \frac{\cos^2(\beta)}{k^2 - 1} \cdot \frac{k \cdot \tan(k\beta) - \tan(\beta)}{\pi} \quad (1)$$

with:

$$\alpha + \beta = \pi \quad (2)$$

where $k = \sqrt{X_C/X_L}$, X_C , X_L , α and β are the reactance of the FC, reactance of the TCR reactor, delay firing angle and conduction angle, respectively. The mentioned equation has been achieved with the assumption that the voltage across the TCSC is non sinusoidal. The TCSC is operated in inductive mode when delay firing angle is the interval $[\pi/2, \alpha_{cri}]$, whereas the capacitive mode is obtained for

$[\alpha_{cri}, \pi]$. α_{cri} is called critical firing angle and can be obtained as follows [2]:

$$\alpha_{cri} = \pi \left(1 - \frac{1}{2k} \right) \quad (3)$$

At the above firing angle, the reactance of TCSC is tended to infinite. Therefore, it is necessary to define an unavailable bound.

3. Proposed local fuzzy based damping controller

3.1. Preliminary remarks

Conventionally, FACTS controllers utilize generators mechanical speed deviations as remote feedback signals to damp the electromechanical oscillations, since such oscillations directly observable from mechanical speed [20]. Remote signals which are available via WAMS, can be used for effectively damping of electromechanical oscillations through WACs. Unavailability of communication infrastructures is the main problem of such method. Moreover, the communication channel inherently causes a time delay. As a result, a robust damping controller design based on local signals is an interesting work from the practical point of view.

Structure of the proposed LFDC is shown in Fig. 1(a). This controller utilizes a local signal, which can be easily provided from the TCSC installation bus. According to the proposed method, a specific local parameter as a feedback signal is measured from the TCSC bus. This signal is compared with the reference value and the resultant error is applied to the fuzzy controller. Subsequently, the output of the fuzzy controller is the reference value of TCSC reactance. Then, the acquired signal is passed through a lookup table to obtain the delay firing angle. By substituting (2) in (1), X_{TCSC} is expressed as $X_{TCSC} = f(\alpha)$. Then, the lookup table is constructed using this expression. However, (1) is mathematically nonlinear and analytical calculation of $\alpha = f^{-1}(X_{TCSC})$ is impossible. In this study, curve fitting technique is used to overcome the problem. The inductive and capacitive areas are fitted by one and three third-order polynomial curves (totally four curves), respectively as follows:

$$X_{TCSC}(\alpha) = a_1 \alpha^3 + a_2 \alpha^2 + a_3 \alpha + a_4 \quad (4)$$

The coefficients a_k , ($k = 1, \dots, 4$) are given in Appendix. It should be noted that all of the above equations are strictly ascending/descending and their inverse can be easily calculated.

Various signals such as active power flowing through the line, frequency and voltage at the TCSC installed bus can be used as an input for the fuzzy controller. The electromechanical oscillations are observable through the electrical frequency and hence this paper proposes the local electrical frequency as the input signal for the LFDC.

To verify the performance of the proposed LFDC, the WFDC is also employed which is based on wide-area measurements. In this sense, the generator speed is measured and transmitted to the TCSC bus by a communication channel. The diagram of the WFDC scheme is shown in Fig. 1(b).

In order to design the fuzzy controller in such a nonlinear system consists of TCSC, generators and transformers, the trial-and-error method is conventionally adopted [21]. However, optimum design of the controller may not be obtained by this method. Heuristic techniques provide intelligent trial-and-error procedures, and hence, in this paper the chaotic optimization algorithm (COA) is adopted in order to optimal design of the fuzzy controller.

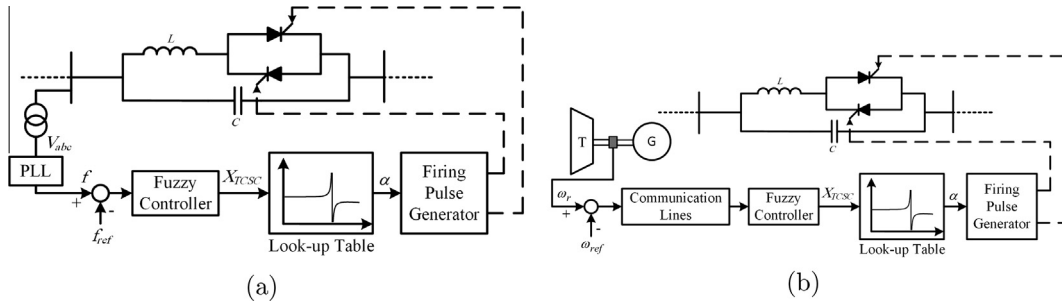


Fig. 1. Structure of (a) proposed local fuzzy based damping controller (LFDC) and (b) wide-area fuzzy based damping controller (WFDC).

3.2. Fuzzy controller

This method is based on fuzzy rules, which can be obtained by the knowledge of expert people. Among various applications of fuzzy logic, fuzzy controller is greatly employed in the literature. This controller is very suitable for control, estimation and optimization of complex nonlinear dynamic systems [21].

The structure of fuzzy controller is shown in Fig. 2(a). The inputs of the fuzzy controller are TCSC local frequency error signal and its changes (or derivative), and its output is the reference (or desired) value of X_{TCSC} . The membership function of inputs/output and the nonlinear surface of error are shown in Fig. 2(b) and (c), respectively. In Fig. 2(c), e and ce denote the error and its changes. The output and each of the inputs are described by seven membership functions in the following way: NB (Negative Big), NM (Negative Medium), NS (Negative Small), Z (Zero), PS (Positive Small), PM (Positive Medium), and PB (Positive Big). The membership functions are considered in the normalized form. For the sake of normalization, the inputs multiplied by two coefficients K_1 and K_2 , and the output multiplied by coefficient K_3 to obtain the actual value of X_{TCSC} . Determination of proper values for these coefficients strongly impresses the operation of the fuzzy controller. The matrix of fuzzy rules is given in Table 1. This matrix is created by 7×7 rules because the inputs are labeled by 7 membership functions.

3.3. Chaotic optimization algorithm

Many problems such as optimal design of fuzzy controller in the complex nonlinear power systems, can be treated as an optimization problem.

Table 1
Matrix of fuzzy rules.

ce	e						
	NB	NM	NS	Z	PS	PM	PB
NB	NB	NB	NB	NB	NM	NS	Z
NM	NB	NB	NB	NM	NS	Z	PS
NS	NB	NB	NM	NS	Z	PS	PM
Z	NB	NM	NS	Z	PS	PM	PB
PS	NM	NS	Z	PS	PM	PB	PB
PM	NS	Z	PS	PM	PB	PB	PB
PB	Z	PS	PM	PB	PB	PB	PB

Global optimum detection is one of the important factors in optimization algorithms. Many heuristic optimization algorithms have been introduced in technical literature such as genetic algorithm (GA), particle swarm optimization (PSO), simulated annealing (SA) and chaotic optimization algorithm (COA), which try to find the global optimal point.

Chaotic behavior is a bounded unstable motion of the deterministic systems in the finite phase space, which has following properties: sensitivity to initial condition, semi-stochastic nature and ergodicity. The main concept of COA is based on applying chaotic process instead of random process in an optimization algorithm, whereby it can be experimentally proven that the search speed is significantly increased. The main features of COA are as follows [22,23]:

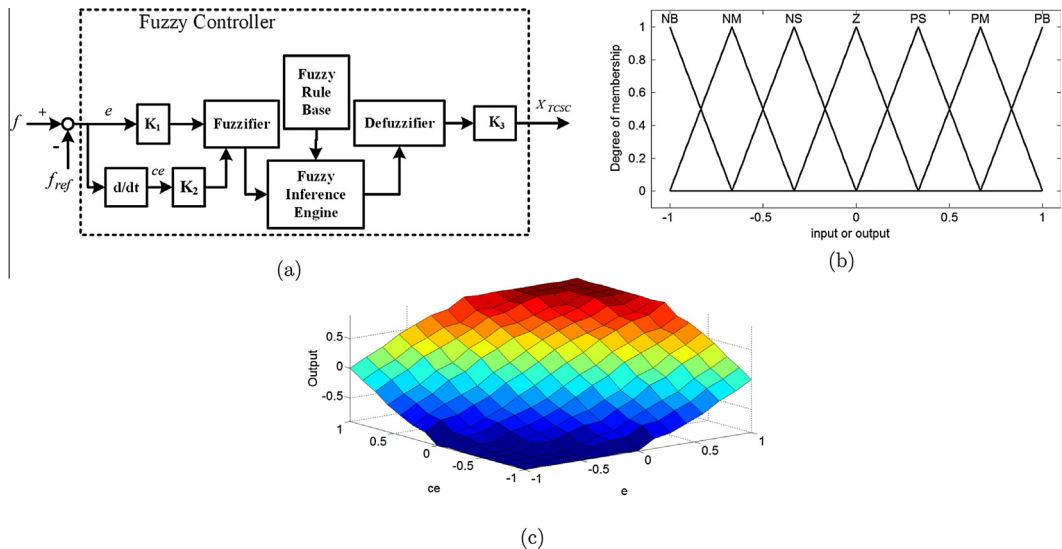


Fig. 2. Fuzzy controller: (a) structure, (b) membership function of inputs/output and (c) nonlinear surface of error.

- It distinguishes between local and global optimal points by its inherent powerful structure.
- It does not produce repetitive numbers in searching progress.
- It is easily implemented and its running time is fairly short.

The COA usually has two main steps as follows [22]:

- Step 1: Mapping a generated sequence of chaotic points from the chaotic space to the solution space and then providing the current optimum point with respect to the objective function.
- Step 2: Obtaining the global optimal point using the current optimal point and chaotic dynamics.

In this paper, the tuning problem of fuzzy controller parameters is converted to an optimization problem which is solved by COA based on Lozi map [24]. The chaotic search procedure based on the Lozi map can be divided into three following steps: initialization of variables and initial conditions, chaotic local search algorithm, and chaotic global search algorithm. Additional information about COA used in this study, including mathematical formulation, and details of chaotic search procedure (local and global search) based on Lozi map are given in [24].

4. Case studies

The utilized model of synchronous generator is based on the model in MATLAB Sim PowerSystems tool box. This model consists of six electrical equations (i.e. Eqs. (5)–(10)) and two mechanical equations (i.e. (12) and (13)). For electrical equations, the stator winding flux in d and q -axis, field winding flux in d -axis, one damper winding flux in d -axis and two dampers winding flux in q -axis have been considered. Also, the two mechanical equations are provided using the separated swing equation with both rotor speed and rotor angle parameters.

The equations of electrical part of the generator (including the dynamics of stator, field, and damper windings) are written as follows [25]:

$$V_d = R_s i_d + \frac{d}{dt} \psi_d - \omega_r \psi_q \quad (5)$$

$$V_q = R_s i_q + \frac{d}{dt} \psi_q + \omega_r \psi_d \quad (6)$$

$$V'_{fd} = R'_{fd} i'_{fd} + \frac{d}{dt} \psi'_{fd} \quad (7)$$

$$V'_{kd} = R'_{kd} i'_{kd} + \frac{d}{dt} \psi'_{kd} \quad (8)$$

$$V'_{kq1} = R'_{kq1} i'_{kq1} + \frac{d}{dt} \psi'_{kq1} \quad (9)$$

$$V'_{kq2} = R'_{kq2} i'_{kq2} + \frac{d}{dt} \psi'_{kq2} \quad (10)$$

The linkage fluxes are related to the currents by:

$$\begin{bmatrix} \psi_q \\ \psi_d \\ \psi'_{kq1} \\ \psi'_{kq2} \\ \psi'_{fd} \\ \psi'_{kd} \end{bmatrix} = \begin{bmatrix} L_q & 0 & L_{mq} & L_{mq} & 0 & 0 \\ 0 & L_d & 0 & 0 & L_{md} & L_{md} \\ L_{mq} & 0 & L'_{kq1} & L_{mq} & 0 & 0 \\ L_{mq} & 0 & L_{mq} & L'_{kq2} & 0 & 0 \\ 0 & L_{md} & 0 & 0 & L'_{fd} & L_{md} \\ 0 & L_{md} & 0 & 0 & L_{md} & L'_{kd} \end{bmatrix} \begin{bmatrix} i_q \\ i_d \\ i'_{kq1} \\ i'_{kq2} \\ i'_{fd} \\ i'_{kd} \end{bmatrix} \quad (11)$$

In these equations, symbols V, i, R, ψ, ω and L denote voltage, current, resistance, flux, angular speed and inductance, respectively. Also, subscripts d, q, f, k, s, r and m denote d -axis, q -axis, field winding, damper winding, stator, rotor and magnetizing quantities, respectively. The mechanical equations of the generator can be expressed as follows:

$$\dot{\delta} = \omega - \omega_0 \quad (12)$$

$$\dot{\omega} = \frac{1}{J} (T_m - T_e - D\omega) \quad (13)$$

where δ, J, T_m, T_e and D denote rotor angle, inertia coefficient, mechanical torque, electrical torque and damping coefficient, respectively. The hydraulic turbine and governor block contains a nonlinear model of hydraulic turbine, PID controller for the governor system and servo motor [26]. Moreover, the excitation system is implemented as a voltage regulator according to the IEEE type I model.

In order to verify the performance of the proposed LFDC, the detailed model of TCSC is applied on three different power systems. The first one is a two-area two-machine (TATM) system. The second and third case studies are WSCC three-machine nine-bus and Kundur's two-area four-machine (TAFM) systems, respectively. The single-line diagrams of these case studies which equipped with TCSC, are depicted in Fig. 3(a)–(c). The data of TATM systems are given in Appendix, and also the data of WSCC and TAFM systems are presented in [27,8], respectively.

In WSCC system, the TCSC is located between buses 5 and 10 at the line connecting generators 1 (swing generator) and 2. In the LFDC strategy the local frequency is measured from bus 5 (TCSC bus), while in the WFDC the rotor speed difference of generators 1 and 2 is considered as the input control signal of TCSC controller. Similarly, in the TAFM test system the TCSC is installed on the tie-line between buses 8 and 12. For LFDC scheme the local frequency is measured at bus 8 (TCSC bus), whereas in WFDC scheme the rotor speed difference of generators 1 and 4 is the input control signal. It is worth to mention that in the TAFM system, the machines located at one side of the tie-line oscillating against the groups of machines on the other side. Thus, generators 1 and 2 are coherent machines which are oscillating against the other set of coherent machines, i.e. generators 3 and 4 at the opposite area. Hence, the speed difference of two non-coherent machines is a desired feedback signal for WFDC. Therefore, in TAFM system the speed difference of generators 1 and 4 is selected arbitrarily, where almost similar results are observed for other selections (e.g. speed difference of generators 1 and 3, 2 and 3 or 2 and 4).

In this paper, in order to keep the comprehensiveness of the study, various types of faults (including single-phase, double-phase and three-phase to ground) are simulated. In TATM system, temporary faults are occurred close to the transformer high voltage bus (see Fig. 3(a)) at $t = 3$ s. In the WSCC and TAFM systems, the faults are occurred at the buses 8 and 7 (see Fig. 3(b) and (c)) at $t = 1$ s, respectively. A duration of 6 cycles for all temporary faults is considered. It is assumed that the faults are cleared by themselves, without manipulation of the system configuration. The WSCC system is inherently stable for all above fault types. But, the TATM system is unstable for both double-phase and three-phase to ground faults, and the TAFM system is unstable for all fault types.

5. Simulation results

In order to investigate the effectiveness of the proposed LFDC, its behavior is compared with WFDC for all above test systems. For this aim, three different indices are introduced as follows,

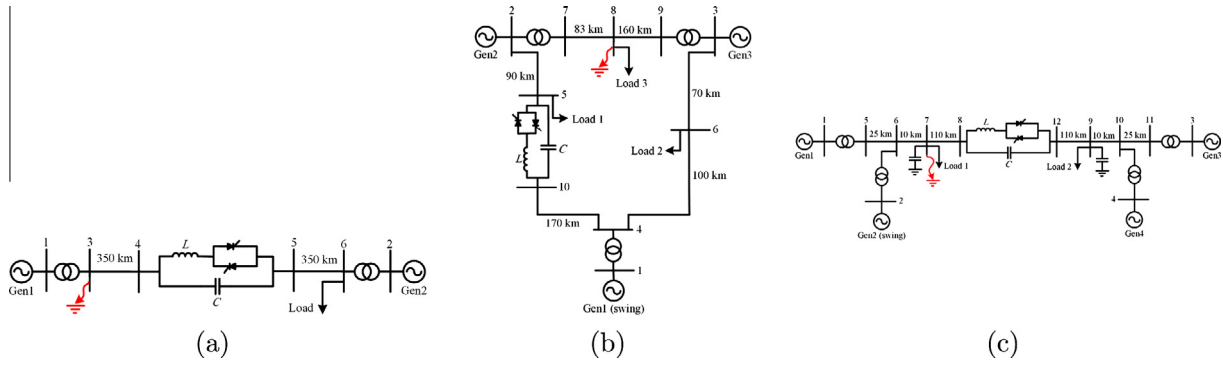


Fig. 3. The case studies: (a) TATM, (b) WSCC and (c) TAFM.

which can easily quantify the performance of both control schemes.

- Index-1: The integral of the time-multiplied absolute value of the error (ITAE) in the following way:

$$ITAE = 1000 \int_0^{t_{sim}} t |\Delta\omega| dt \quad (14)$$

where t_{sim} is the simulation time and $\Delta\omega$ is the rotor speed difference. ITAE integrates the absolute $\Delta\omega$ multiplied by the time, over time. The t representing time under the integral, penalizes long duration of speed differences. In the case studies, $\Delta\omega = \omega_{gm} - \omega_{gn}$, where m and n are the generator numbers. In the TATM system $m = 1, n = 2$, whereas in the WSCC system $m = 1, n = \{2, 3\}$ and in the TAFM system $m = 1, n = 4$.

- Index-2: The maximum load angle which is demonstrated by δ_{mn}^{max} .
- Index-3: The settling time (T_s) of the rotor speed difference $\Delta\omega$. In this regard, the 5% criterion is adopted.

Since in the WFDC scheme the control signal is provided from wide-area measurements via a communication infrastructure, it is necessary to investigate the deficiencies of this system, such as the communication delays and channel failure. Hence, the following impact of communication delays and failure on the WFDC scheme, are also studied.

Also, to emphasize on the impact of detailed model of TCSC on the system performance, another comparison is made between the detailed and phasor models of TCSC, in the TATM power system. All numerical simulations are carried out by Matlab/Simpower toolbox.

5.1. Case 1: the TATM system

In this section, the performance of the proposed LFDC and WFDC is evaluated in the TATM power system. In order to precisely assessment of the aforementioned controllers, the simulation results are also compared with another wide-area measurement-based damping control strategy, named "Bang-Bang" control. At first, this control strategy was proposed in [28] for the design of SVC and STATCOM damping controllers. In this paper Bang-Bang damping controller (BBDC) which is a mixed discrete–continuous controller is employed for TCSC as follows:

$$X_{TCSC}(t) = \begin{cases} X_C & \Delta\omega \geq 0, t \leq T_C \\ X_L & \Delta\omega < 0, t \leq T_C \\ k_{TCSC}\Delta\omega(t) & t > T_C \end{cases} \quad (15)$$

where T_C is the instant in which the control switches from the discrete to continuous mode. Also, k_{TCSC} is a positive constant gain and

its value is assumed to be $k_{TCSC} = 50$ here. It should be noted that the described control strategy is clearly based on the wide-area signals (i.e. the speed difference of remote generators).

Fig. 4 illustrates the load angle and rotor speed difference in single-phase, double-phase and three-phase to ground faults for the LFDC, WFDC and BBDC in the TATM power system. Regarding Fig. 4 and Table 2, from the view point of Index-1 and Index-2, although the WFDC and BBDC controllers are slightly better than the proposed LFDC, but all of them are approximately similar from the Index-3 perspective. It means that, the damping capability of the proposed LFDC scheme for all types of faults is fairly comparable with WFDC and BBDC. As a result, although the maximum load angle for LFDC is higher than WFDC and BBDC, but the oscillations are damped in the same time.

5.2. Case 2: the WSCC system

The rotor speed differences of WSCC test system in the presence of TCSC equipped with the proposed LFDC and WFDC are illustrated in Fig. 5. Also, the values of indices are listed in Table 3. In this table, the indices are calculated for speed differences of generators 1 and 2 (denoted by G_{12}) and generators 1 and 3 (denoted by G_{13}). In the WFDC scheme, rotor speed difference of generators 1 and 2 is considered as the wide-area control signal, since the TCSC is located between these generators. Regarding Fig. 5 and Table 3, it can be inferred that the proposed LFDC is just slightly weaker than the WFDC from the viewpoint of all indices. Previously mentioned, since the rotor speed difference is more observable and controllable than the local frequency, the obtained results by LFDC are reasonable. On the other hand, in real power system due to several problems such as communication infrastructure failure and time delay of WFDC scheme, the LFDC can be deployed as an effective alternative. This is previously concluded for TATM system and here is confirmed for a larger system.

In WSCC system with TCSC controlled by WFDC, the proper choice of wide-area control signal has significant impact on the electromechanical oscillations damping, due to the asymmetric structure of the system. Usually, wide-area signals of two generators which TCSC is located between them, have better results. Accordingly, in this study, since the TCSC is installed between generators 1 and 2, the rotor speed difference between these generators is used in WFDC scheme. With this selection, the relative oscillations of remaining generator (i.e. generator 3) has higher amplitude than the ones of these two generators.

5.3. Case 3: the TAFM system

The results obtained by the proposed LFDC and WFDC for TAFM system are presented in Fig. 6 and Table 4. In the WFDC scheme the

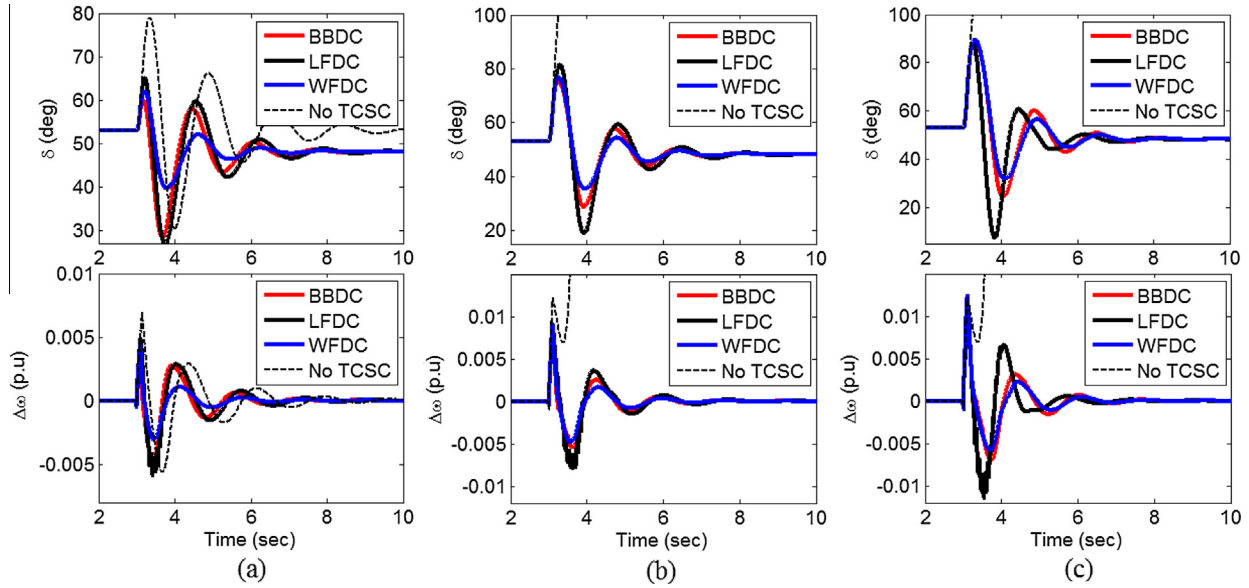


Fig. 4. The operation of the LFDC, WFDC and BBDC schemes in the TATM power system under: (a) single-phase, (b) double-phase and (c) three-phase to ground faults.

Table 2
The values of indices for TATM system.

Control scheme	Fault type	Index-1	Index-2	Index-3
LFDC	1 ϕ	23.66	65.20	6.10
	2 ϕ	31.97	81.40	6.20
	3 ϕ	36.08	88.30	4.40
WFDC	1 ϕ	10.18	62.20	4.50
	2 ϕ	18.56	76.80	4.70
	3 ϕ	26.18	89.60	4.80
BBDC	1 ϕ	18.62	60.00	5.90
	2 ϕ	23.71	75.40	4.70
	3 ϕ	32.10	87.90	6.20
No TCSC	1 ϕ	33.53	79.17	6.50
	2 ϕ	Unstable	Unstable	Unstable
	3 ϕ	Unstable	Unstable	Unstable

formance of the LFDC scheme on the basis of three defined indices is close to the WFDC scheme. In this system, from the perspective of Index-3, capability of the LFDC is slightly better than the WFDC, i.e. the system has lower settling time. Eventually, with regard to the all results, the proposed LFDC could be utilized as an appropriate alternative for WFDC.

5.4. The impact of communication delays and failure on the performance of WFDC

In this section, the impacts of communication delays along with its failure are investigated in WSCC and TAFM systems for different types of communication links. In Ref. [29] the typical delay times of various communication links are reported which are employed in WFDC scheme for the sake of comparison with the proposed LFDC. Also, in order to model the communication failure, it is assumed that the channel is unavailable (or fails) for about 1 s, at $t = 1$ s (i.e. the communication channel is unavailable in the interval [1, 2] s). For the sake of brevity, the simulations are carried out only

indices are calculated for rotor speed difference of generators 1 and 4, since these generators are not coherent machines, and located at the opposite areas. Similar to previous three case studies, the per-

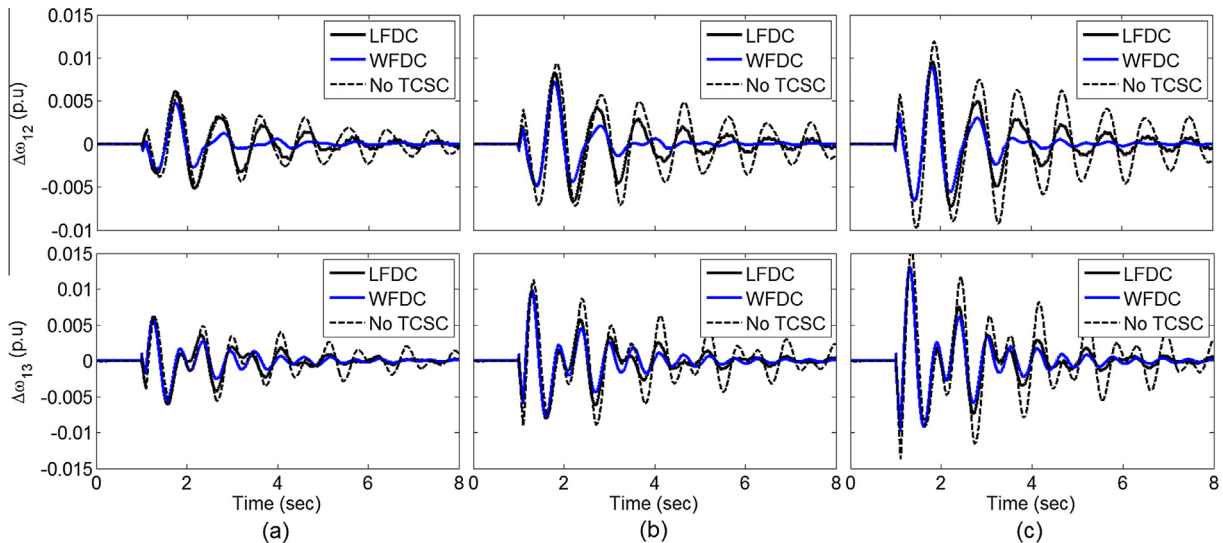


Fig. 5. The rotor speed differences for WSCC system using LFDC and WFDC schemes under: (a) single-phase, (b) double-phase and (c) three-phase to ground faults.

Table 3
The values of indices for WSCC system.

Control scheme	Fault type	Index-1		Index-2		Index-3	
		G_{12}	G_{13}	G_{12}	G_{13}	G_{12}	G_{13}
LFDC	1 ϕ	26.56	20.43	54.31	54.87	7.47	6.87
	2 ϕ	36.07	29.52	59.64	59.16	7.34	6.83
	3 ϕ	42.93	37.11	62.73	64.75	7.39	6.87
WFDC	1 ϕ	9.75	14.38	45.74	51.53	5.67	5.89
	2 ϕ	13.93	22.77	51.67	53.48	3.91	5.15
	3 ϕ	18.98	29.41	56.24	64.76	4.59	5.16
No TCSC	1 ϕ	47.16	40.92	51.39	57.31	>8	>8
	2 ϕ	75.57	66.64	60.39	64.13	>8	>8
	3 ϕ	97.99	87.12	66.95	74.92	>8	>8

for three-phase to ground fault, which is already the most severe fault in both cases.

Fig. 7(a) shows the variation of relative load angles and rotor speed difference (between generators 1 and 2) in WSCC system for different values of communication delay and failure. It is observed from this figure that when the delay increases, the damping of oscillations decreases correspondingly. For the delays of 300 ms and 700 ms, the performance of WFDC falls below the LFDC scheme, since undamped low frequency electromechanical oscillations are observed in the presence these delays.

On the other hand, it is clear when a communication failure is occurred for duration of 1 s, the performance of WFDC is deteriorated. For larger durations of the failure (in this case, 1.7 s) the system will be unstable for the same fault.

For above two cases, the value of performance indices are given in Table 5. It is inferred from this table that by increasing the delay time, all indices start to become worse. This is more salient for Index-1 and Index-3. These indices reflect directly the damping of electromechanical oscillations.

Similarly, for the same values of communication delays and failure, the obtained results for the TATM system are also given in Fig. 7(b) and Table 6. It is evidently observed that the larger amounts of delay, reduce the damping capability of WFDC scheme, where by increasing the delay to 700 ms, the system tends to instability. Besides, the communication failure of 1 s, increases both the amplitude of oscillations and settling time in the case of WFDC. Similar to the WSCC case, it is observed that the failure causes the deterioration of WFDC performance, where the system is

Table 4
The values of indices for TAFM system.

Control scheme	Fault type	Index-1	Index-2	Index-3
	2 ϕ	20.51	52.62	3.92
	3 ϕ	22.05	55.32	3.98
WFDC	1 ϕ	11.18	44.28	3.80
	2 ϕ	14.27	47.71	4.02
	3 ϕ	17.49	51.71	4.03
No TCSC	1 ϕ	Unstable	Unstable	Unstable
	2 ϕ	Unstable	Unstable	Unstable
	3 ϕ	Unstable	Unstable	Unstable

unstable for failure durations larger than 1.5 s. Table 6 summarizes the impact of various communication delays and channel failure on the performance indices. It is observed from this table that the delays influence mainly Index-1 and Index-3, which these indices directly reflect the damping capability of WFDC controller.

5.5. Comparison of detailed and phasor models of TCSC in TATM system

Utilization of the detailed model of TCSC (via (1) and (2)) is one of the contributions of this paper. However, to evaluate transient stability of power systems in the presence of TCSC, most of the previous studies used approximate phasor model, instead. In the phasor model, the TCSC is modeled by a current controlled voltage source. In this way, first the reference value of TCSC reactance is obtained by aforementioned control strategy (see Fig. 1(b)). Then, the TCSC voltage is calculated as $V_{TCSC} = jX_{TCSC}I_{TCSC}$, where X_{TCSC} and I_{TCSC} are the reference values of the TCSC reactance and the line (or TCSC) current, respectively.

The comparison of detailed and phasor models of TCSC in WFDC scheme is carried out in the TATM system. The load angle and rotor speed difference of generators 1 and 2 are illustrated in Fig. 8(a) for single-phase to ground fault. Similarly, Fig. 8(b) illustrates the result for three-phase to ground fault. The simulation results show that the transient behavior of the detailed and phasor models is significantly different. The oscillations of rotor speed difference in the detailed model is more than the phasor model for both faults. Consequently, if phasor model is utilized for TCSC, the designed damping controller yields optimistic results. However,

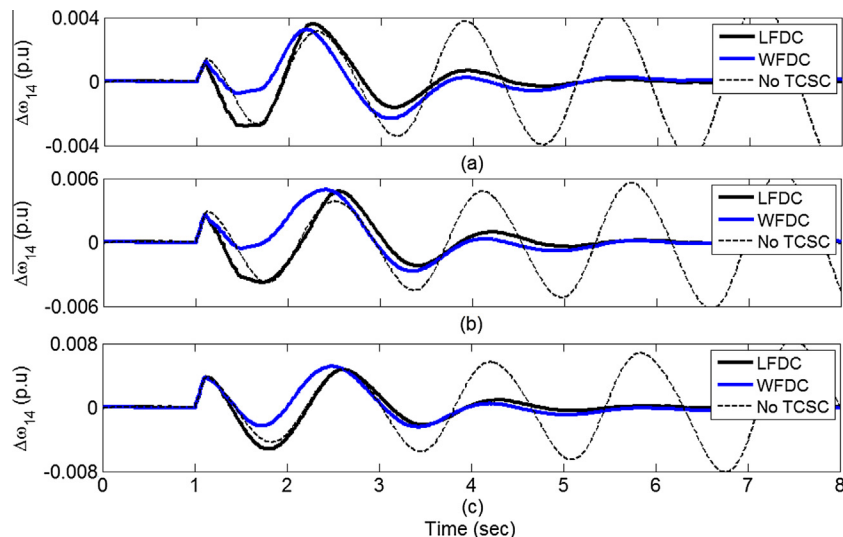


Fig. 6. The rotor speed deviation for TAFM system using LFDC and WFDC schemes under: (a) single-phase, (b) double-phase and (c) three-phase to ground faults.

Table 5
The values of indices in WSCC system, for different communication links delays and its failure.

Control scheme	Communication link	Delay time (s)	Index-1	Index-2	Index-3
WFDC	No delay	–	18.98	56.24	4.59
	Fiber-optic cables [29]	0.15	29.61	60.48	5.25
	Power line communication (PLC) [29]	0.30	101.4	65.27	>8
	Satellite link [29]	0.70	107.4	63.73	>8
	Communication failure	–	26.66	61.22	4.75
LFDC	–	–	42.93	62.73	7.39

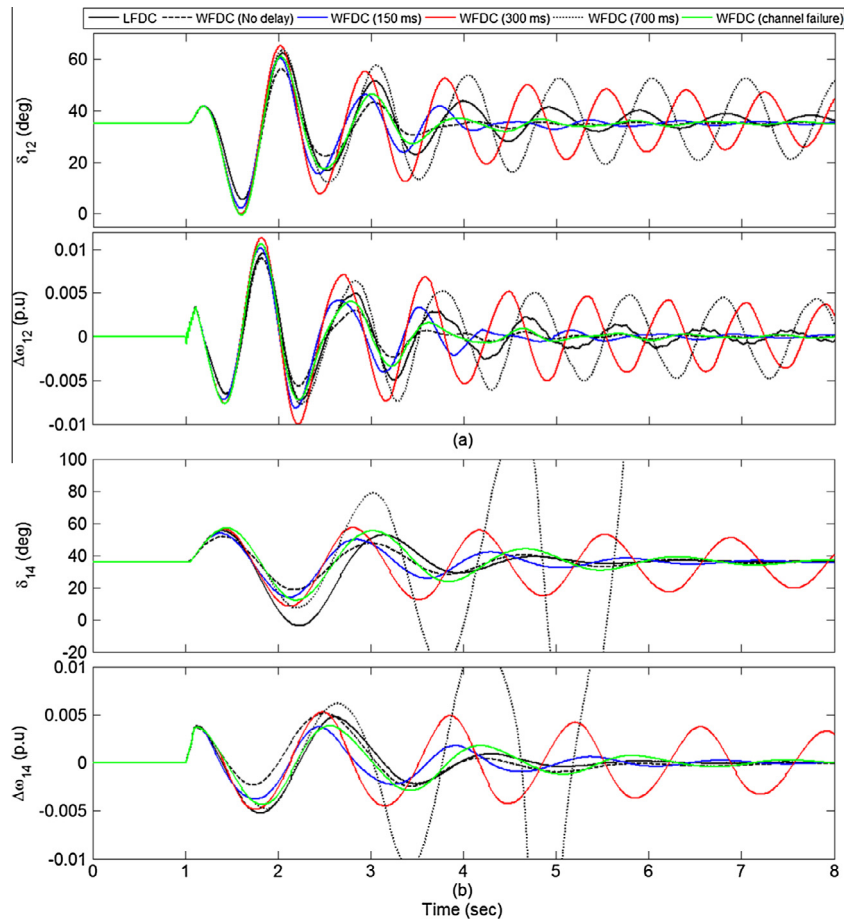


Fig. 7. The impact of communication delays and failure under three-phase to ground fault in (a) WSCC and (b) TAFM system.

Table 6
The values of indices in TAFM system, for different communication links delays and its failure.

Control scheme	Communication link	Delay time (s)	Index-1	Index-2	Index-3
WFDC	No delay	–	17.49	51.71	4.03
	Fiber-optic cables [29]	0.15	21.75	53.80	6.91
	Power line communication (PLC) [29]	0.30	79.37	56.40	>8
	Satellite link [29]	0.70	Unstable	Unstable	Unstable
	Communication failure	–	27.08	56.90	5.51
LFDC	–	–	22.05	55.32	3.98

the obtained results are inaccurate for the practical implementation.

6. Conclusions

This paper deals with improvement of electromechanical oscillations damping in power systems, by proper control of TCSC

equivalent reactance. For this purpose, LFDC scheme is introduced which uses the local frequency at the TCSC installed bus as the input control signal. In the proposed LFDC, the COA is adopted to determine the optimum values of fuzzy controller gains as an intelligent trial-and-error process. The main characteristics of LFDC are compared with WFDC and BBDC by numerical simulations performed on TATM, WSCC and TAFM power systems. Three perfor-

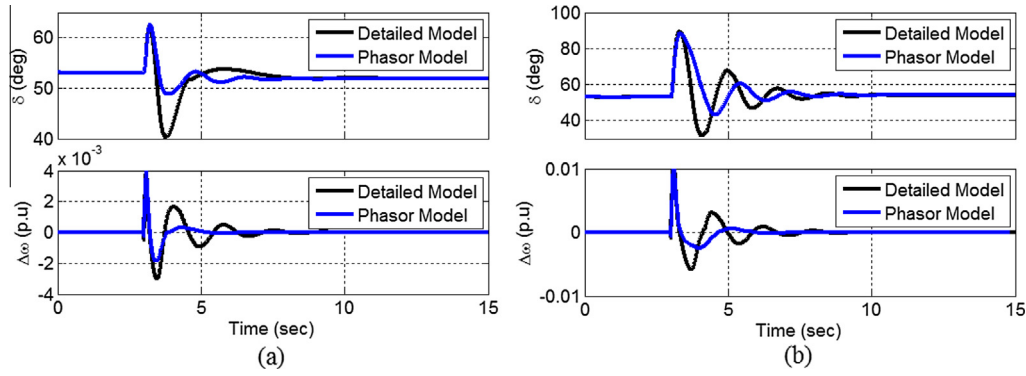


Fig. 8. Comparison of detailed and phasor models of TCSC in TATM system (for WFDC scheme), under: (a) single-phase and (b) three-phase to ground faults.

Table 7
The parameters of TATM case studies.

Parameter description	Symbol	Value
<i>Rated values</i>		
Frequency (Hz)	f	60
Rated power (MVA)	P_n	$G_1 = 1000$ and $G_2 = 5000$
Rated voltage (kV)	V_n	13.8
<i>Synchronous generators</i>		
Inertia constant (s)	H	3.7
Stator resistance (pu)	R_s	0.00285
d-axis subtransient reactance (pu)	X''_d	0.252
d-axis transient reactance (pu)	X'_d	0.296
d-axis synchronous reactance (pu)	X_d	1.035
q-axis subtransient reactance (pu)	X''_q	0.243
q-axis synchronous reactance (pu)	X_q	0.474
d-axis subtransient time const (pu)	T''_{do}	0.053
d-axis transient time const (pu)	T'_{do}	1.01
q-axis subtransient time const (pu)	T''_{qo}	0.1
Armature leakage reactance (pu)	X_a	0.18
<i>Line data</i>		
Line resistance (Ω)	R_l	12.285
Line reactance (Ω)	X_l	230.44
<i>Hydraulic turbine governor</i>		
Servo motor gain	K_a	3.33
Servo motor time constant (s)	T_a	0.07
Permanent droop	R_p	0.05
Regulator proportional gain	K_p	1.163
Regulator integral gain	K_I	0.105
LPF time constant (s)	T_d	0.01
Water starting time (s)	T_w	2.67
Damping coefficient	β	0
<i>Excitation system</i>		
LPF time constant (s)	T_r	0.02
Regulator gain	K_A	300
Regulator time constant (s)	T_A	0.001
Damping filter gain	K_f	0.001
Damping filter time constant (s)	T_f	0.1
<i>TCSC parameters</i>		
TCSC capacitive reactance (Ω)	X_C	20 (TATM and TAFM) and 40 (WSCC)
Reactance ratio	$\frac{x_l}{X_C}$	0.133

mance indices, i.e. ITAE, maximum load angle and settling time of rotor speed are introduced for this aim.

It is worth to note that WFDC and BBDC suffer from multiple problems such as communication infrastructures failure and delays. Hence, the performance of LFDC scheme is compared with WFDC in WSCC and TAFM systems, in terms of communication delays and failure. It is also observed that contrary to LFDC scheme, the performance of WFDC is highly affected by the delay time, in

which the larger the communication delays, both the higher amplitude of oscillations and settling time.

In the case of communication channel failure, it is observed in both systems that contrary to LDFC scheme, the performance of WFDC tends to deteriorate when failure duration increases. Even, for durations larger than a specific threshold in each case, the systems are unstable. As a result, the proposed LFDC scheme could be a proper alternative for wide-area measurement based controllers

such as WFDC and BBDC, since the aforementioned problems are not likely to occur, in the case of local measurement-based controllers.

Moreover, in this paper, the nonlinear detailed model of TCSC is employed and its performance is compared with the widely used phasor model. The comparison results show that the behavior of system considering the detailed model of TCSC is completely different from the phasor model.

Appendix A

A.1. Polynomial curve fitting of X_{TCSC}

The inverse of (1) is not accessible mathematically. Thus, to acquire the inverse of (1), this paper divides the TCSC reactance curve into four parts. For this purpose, at the first, ascendance or descentance of X_{TCSC} curve must be considered using derivative of $X_{TCSC}(\beta)$. According to Derivative of (1), only one part of X_{TCSC} is ascending. In addition, although for $14.71^\circ \leq \beta \leq 32.18^\circ$ derivative of (1) is descending, but X_{TCSC} cannot be accurately approximated by third-order polynomial. Consequently, this part is divided into two different areas. Hence, the capacitive mode of X_{TCSC} contains three different parts and the inductive mode has only one part. Using the curve fitting technique of MATLAB, the approximate characteristic of TCSC reactance versus to the conduction angle is given by (A.1).

To obtain the mentioned equation versus firing angle, Eq. (2) could be used. It should be noted that the range between 32.18 and 60 for conduction angle is defined as forbidden or unavailable band.

A.2. The parameters of TATM case study

The parameters of TATM test system (including synchronous generator, transmission line, hydraulic turbine governor, excitation system and TCSC parameters) are given in Table 7.

$$X_{TCSC}(\beta) = \begin{cases} -0.00035603\beta^3 + 0.001835\beta^2 + 0.18942\beta - 19.994 & 0 < \beta \leq 14.71 \\ -0.0082774\beta^3 + 0.43411\beta^2 - 7.702\beta + 27.982 & 14.71 < \beta \leq 27.47 \\ -3.4702\beta^3 + 302.12\beta^2 - 8768.9\beta + 84818 & 27.47 < \beta \leq 32.18 \\ -3.2 \times 10^{-5}\beta^3 + 0.0068614\beta^2 - 0.49162\beta + 14.424 & 60 \leq \beta \leq 90 \end{cases} \quad (\text{A.1})$$

References

- [1] Hingorani NG, Gyugyi L. Understanding FACTS: concepts and technology of flexible ac transmission systems. New York: IEEE Press; 1999.
- [2] Mathur RM, Varma RK. Thyristor-based facts controllers for electrical transmission systems. New York: IEEE Press; 2002.
- [3] Jovcic D, N Pillai G. Analytical modeling of TCSC dynamics. IEEE Trans Power Del 2005;20(2):1097–104.
- [4] Zhao K, Li J, Zhang C, Lee W. Dynamic simulator for thyristor-controlled series capacitor. IEEE Trans Ind Appl 2010;46(3):1096–102.
- [5] Pilotto LAS, Bianco A, Long WF, Edris A. Impact of TCSC control methodologies on subsynchronous oscillations. IEEE Trans Power Del 2003;18(1):243–52.
- [6] Joshi SR, Cheriyan EP, Kulkarni AM. Output feedback SSR damping controller design based on modular discrete-time dynamic model of TCSC. IET Gen Transm Distrib 2009;3(6):561–73.
- [7] Kabiri K, Henschel S, Mart JR, Dommel HW. A discrete state-space model for SSR stabilizing controller design for TCSC compensated systems. IEEE Trans Power Del 2005;20(1):466–74.
- [8] Kundur P. Power system stability and control. New York: McGraw-Hill; 1994.
- [9] Lu C, Hsu C, Juang C. Coordinated control of flexible AC transmission system devices using an evolutionary fuzzy lead-lag controller with advanced continuous ant colony optimization. IEEE Trans Power Syst 2013;28(1):385–92.
- [10] Liu Q, Vittal V, Elia N. LPV supplementary damping controller design for a thyristor controlled series capacitor (TCSC) device. IEEE Trans Power Syst 2006;21(3):1242–9.
- [11] Ali ES, Abd-Elazim SM. Coordinated design of PSSs and TCSC via bacterial swarm optimization algorithm in a multimachine power system. Electr Power Energy Syst 2012;36(1):84–92.
- [12] Chaudhuri B, Pal BC. Robust damping of multiple swing modes employing global stabilizing signals with a TCSC. IEEE Trans Power Syst 2004;19(1):499–506.
- [13] Fang DZ, Xiaodong Y, Wennan S, Wang HF. Oscillation transient energy function applied to the design of a TCSC fuzzy logic damping controller to suppress power system interarea mode oscillations. IEE Proc Gener Transm Distrib 2003;150(2):233–8.
- [14] Hameed S, Das B, Pant V. A self-tuning fuzzy PI controller for TCSC to improve power system stability. Electr Power Syst Res 2008;78(10):1726–35.
- [15] Chatterjee D, Ghosh A. Transient stability assessment of power systems containing series and shunt compensators. IEEE Trans Power Syst 2007;22(3):1210–20.
- [16] Dai XZ, He D, Fan LL, Li NH, Chen H. Improved ANN α -th-order inverse TCSC controller for enhancing power system transient stability. IEE Proc Gener Transm Distrib 1999;146(6):550–6.
- [17] Tan X, Zhang N, Tong L, Wang Z. Fuzzy control of thyristor-controlled series compensator in power system transients. Fuzzy Sets Syst 2000;110(3):429–36.
- [18] Zhang S, Vittal V. Design of wide-area power system damping controllers resilient to communication failures. IEEE Trans Power Syst 2013;28(4):4292–300.
- [19] Yao W, Jiang L, Wu QH, Wen JY, Cheng SJ. Delay-dependent stability analysis of the power system with a wide-area damping controller embedded. IEEE Trans Power Syst 2011;26(1):233–40.
- [20] Yao W, Jiang L, Wen JY, Wu QH, Cheng SJ. Wide-area damping controller of FACTS devices for inter-area oscillations considering communication time delays. IEEE Trans Power Syst 2014;29(1):318–29.
- [21] Gadoue SM, Giauoris D, Finch JW. MRAS sensorless vector control of an induction motor using new sliding-mode and fuzzy-logic adaptation mechanisms. IEEE Trans Energy Convers 2010;25(2):394–402.
- [22] Yang D, Li G, Cheng G. On the efficiency of the chaos optimization algorithms for global optimization. Chaos Solit Fract 2007;34(4):1366–75.
- [23] Yan XF, Chen DZ, Hu SX. Chaos-genetic algorithms for optimizing the operating conditions based on RBF-PLS model. Comput Chem Eng 2003;27(10):1393–404.
- [24] Shayeghi H, Shayanfar HA, Jalilzadeh S, Safari A. Multi-machine power system stabilizers design using chaotic optimization algorithm. Energy Convers Manage 2010;51(7):1572–80.
- [25] Krause PC. Analysis of electric machinery. McGraw-Hill; 1986.
- [26] IEEE working group on prime mover and energy supply models for system dynamic performance studies: 'Hydraulic Turbine and Turbine Control Models for Dynamic Studies'. IEEE Trans Power Syst Feb. 1992;7(1):167–79.
- [27] Sauer PW, Pai MA. Power system dynamics and stability. Englewood Cliffs, NJ, USA: Prentice-Hall; 1998.
- [28] Haque MH. Improvement of first swing stability limit by utilizing full benefit of shunt FACTS devices. IEEE Trans Power Syst 2004;19(4):1894–902.
- [29] Naduvathuparambil B, Valenti MC, Feliachi A. Communication delays in wide area measurement systems. In: Proceedings of the thirty-fourth southeastern symposium on system theory; 2002. p. 118–22.